Analysis of Variable Mass Rotordynamic Systems with Semi-analytic Time-Integration

Helmut J. Holl(✉)

Institute of Technical Mechanics, Johannes Kepler University of Linz,
Altenbergerstraße 69, 4040 Linz, Austria
helmut.holl@jku.at
https://www.jku.at/tmech/holl

Abstract. The analysed rotordynamic system is modeled as a non-linear variable mass system and represents a part of a production line where an axially moving material is coiled on a rotating drum. The suitable and accurate simulation of the vibrations in a coiling process is important to predict the vibrations during standard operation and for special non-steady operation conditions. Variable parameters are present and bending vibrations of the rotor with the coiling drum and the transversal oscillations of the elastic strip are coupled. The longitudinal and transversal motion of the axially moving strip and the bending deflection of the coiling drum are considered by Rayleigh-Ritz approximations which involve the application of the extended equation of Lagrange for open systems. Simulations are performed for a non-linear rotordynamic system for different operation conditions. The results computed with a semi-analytic time-integrations algorithm are shown.

Keywords: Variable mass system · Coiling process
Variable parameters · Extended equation of Lagrange

1 Introduction

For the simulation of the vibrations in a coiling process a suitable mechanical model is necessary. In the coiling process an axially moving strip moves continuously towards a rotating drum where it is coiled. For instance between two successive coiling processes the strip passes through a Steckel mill where the thickness is reduced. In this paper the mechanical model starts at the exit of the Steckel mill and considers the axial motion of the strip with the transversal oscillations. Then the strip is coiled and when the strip is attached to the drum it contributes to the bending stiffness and increases the mass and the outer radius of the drum. As the exact description of the coiling process is very complicated, it is assumed that the coiled strip is fixed on the coiling drum when it touches the drum so that the stiffness of the drum increases with the rotation angle.

K. L. Cavalca and H. I. Weber (Eds.): IFToMM 2018, MMS 62, pp. 412–425, 2019.
https://doi.org/10.1007/978-3-319-99270-9_30

The accumulation of the mass on the coiling drum has a certain influence on the vibrations of the total system during operation. The resulting mechanical model is a non-linear dynamic model with varying mass and system parameters, which are defined by the variable outer radius of the drum, the variable bending stiffness and a variable eccentricity of the rotating drum. Due to the coiled material the mass of the coiling drum increases or decreases continuously. For the outer radius of the coiling drum an Archimedian Spiral is assumed, which gives a position dependent outer radius and bending stiffness of the rotating shaft with the drum. For the simulation of the coiling process with the long computation time a semi-analytic time integration method was implemented.

For the derivation of the equations of motion Rayleigh-Ritz approximations are used to get a minimal number of degrees of freedom in the mechanical model. The application of the extended equations of Lagrange, see [1], is necessary as the mass in the system is not constant, which is a restriction for the well-known equations of Lagrange, see [2]. In the extended equations of Lagrange the control volume concept with the surface integrals with partial derivatives as a kernel are present. The control volume concept for the non-linear dynamic system takes the flow of mass through the boundary into account. For the application of this control volume concept it is important to distinguish between the material control volume and the spatial control volume. If the relative speed between the surface of the control volume and the transported material does not depend on the applied degrees of freedom and their time derivatives, it can be seen from the equations in [1] and also [3] that the surface integral terms vanish and the classical form of the Lagrange equations results. In [4] additionally some literature on dynamic systems with variable mass is cited and in [5–9] different mechanical models with variable parameters have been analysed. In [10,11] an alternative approach for the influence of the variable mass is considered using reactive forces, where also some examples are discussed and the effect of the reactive force is studied for the case of winding up a band. A model for an industrial application with additional strip guiding rolls was analysed in [7,8], where the strip tension force was computed for a given entrance speed of the strip. In [12,13] the effect of the time variable eccentricity is considered where the time derivatives of the eccentricity are involved and it is shown that very small vibration amplitudes result.

The temperature of the coiled strip is usually not constant over the long process time, so that a thermal deflection of the shaft of the coiling drum can occur due to a certain non-homogeneous temperature distribution. The thermal deflection represents a kinematic parameter in the mechanical model and has a high influence on the strip tension force. The strip tension force is a critical process parameter which should be constant and at least should be positive. The effect of the thermal deflection of the coiling drum results in high vibration amplitudes which was analysed in [9] for the uncoupled system where computed results are shown for the controlled system with thermal deflection. Predeformation or misalignment of the shaft can be caused by production tolerances, inhomogeneous temperature distribution or maintenance errors. In this paper the coupled vibrations are analysed and numerical studies are performed in order to increase the knowledge about the complicated variable mass non-linear dynamic system of the coiling drum and the axially moving strip. For the dynamic system the initial and boundary conditions are defined and with the defined operation conditions a developed semi-analytic time-integration algorithm computes the solution. An algorithm was used which has been presented in [5,14] and has been extended in [15] to substructure analysis.

2 Mechanical Modelling of the Coiling Process

The mechanical model of the coiling process includes the coiling drum on elastic shaft in rigid bearings and the moving strip, see Fig. 1. Rayleigh-Ritz approximations and the extended equations of Lagrange have been used for the derivation of the mechanical model. The resulting mechanical model has five degrees of freedom, the horizontal and vertical deflection x, y, the rotation angle φ of the coiling drum, the transversal deflection of the moving strip q and the entrance speed of the strip $\dot{s}_L$. The strip tension force F_B is given as a predefined value at the entrance of the system. The torque at the coiling drum M_T is controlled to maintain a suitable process.

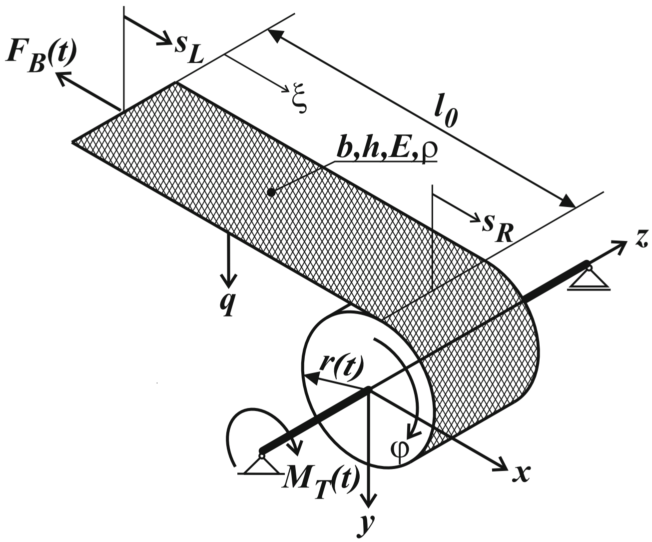

Fig. 1. Mechanical model of the rotating drum with the axially moving strip

For the derivation of the equations of motion it is important to distinguish between the material control volume and the spatial control volume, see [1]. The spatial control volume is an arbitrary moving non-material volume with a surface that has a speed **w** which is different from the velocity of the material at the surface $\mathbf{v}$. The transport of kinetic energy and mass can be determined and is related to the spatial derivative of the total kinetic energy at the boundary of the control volume so that the extended equation of Lagrange, see [1], can be written in the form

$$\frac{d}{dt}\left(\frac{\partial T}{\partial \dot{q}_i}\right) - \frac{\partial T}{\partial q_i} + \frac{1}{2}\oint_{\partial V_i} \frac{\partial \mathbf{v}^2}{\partial \dot{q}_i}\rho\left(\mathbf{v}-\mathbf{w}\right)\mathbf{n}dS - \oint_{\partial V_i} \rho\frac{\mathbf{v}^2}{2}\frac{\partial\left(\mathbf{v}-\mathbf{w}\right)}{\partial \dot{q}_i}\mathbf{n}dS = Q_i, \quad (1)$$

where $\mathbf{n}$ is the outward normal vector at the boundary of the control volume. The control volume of the mechanical system can be seen in Fig. 2. The surface integral terms vanish if the velocity at the boundary of the control volume are prescribed and independent of the degrees of freedom q_i of the system.

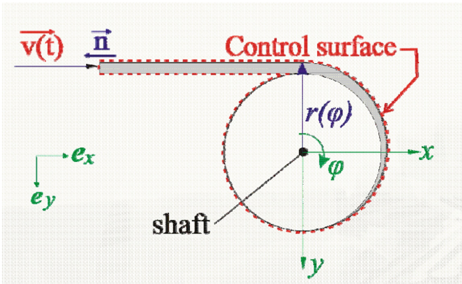

Fig. 2. Control Volume for the Mechanical model of the rotating drum with the axially moving strip

2.1 Model of the Coiling Drum

The coiling drum is modeled as a beam with varying bending stiffness. In a first step the outer radius of the drum increases in accordance to an Archimedian spiral

$$r = r_0 + \frac{h\varphi}{2\pi}, \quad (2)$$

where h is the thickness of the strip. For the actual bending stiffness of the rotating shaft it is assumed that the coiled strip is attached to the drum and contributes to the stiffness. The total mass of the coiling drum is $m_C = m_0 + \rho A s_R$ and its time derivative is $\dot{m}_C = \rho A \dot{s}_R$, where ρ is the density of the strip material, A is the cross section of the strip, s_R is the coiled length of the strip and $\dot{s}_R$ its time derivative.

The mechanical system of the coiling drum, which is considered in this paper, is shown in Fig. 1. The equations of motion are written in the coordinates of the center of the shaft. The exact position of the center of gravity of the coiling drum including the strip changes during the coiling process and can be computed according to the results shown in [12,13]. Because of the symmetry in the mechanical model we consider vibrations of the coiling drum in the x-y-plane only. At the coiling drum the torsion moment M_T is applied, b is the width of the strip and h is the strip thickness. $\dot{s}_L$ is the entrance speed of the strip and $\dot{s}_R$ is the absolute speed of the strip when attaching the coiling drum. The coiling drum rests on rigid bearings, so that only the stiffness of the shaft is taken into account. It is assumed that the thermal deflection is caused by a non-homogeneous temperature distribution within the coiling drum and results in a total deflection a which is measured in the mid-plane of the drum. The actual coordinates of the center of gravity of the drum are denoted by x_S and y_S, whereas for the center of the shaft the coordinates denoted by x_W and y_W are used. Due to the thermal deflection the position of the center of the undeformed shaft was defined by x_{W0} and y_{W0}. In the following computations the strip tension force $F_B(t)$ is predefined and the resulting model has five degrees of freedom x_W, y_W, φ, q_i and s_L. In the special case with a prescribed speed $\dot{s}_L$ at the left boundary, the mechanical model results in four degrees of freedom which is not considered here.

The kinetic energy of the coiling drum is computed by

$$T_C = m_C \frac{\dot{x}_S^2 + \dot{y}_S^2}{2} + J_C \frac{\dot{\varphi}^2}{2} \tag{3}$$

with the momentum of inertia defined by

$$J_C = \frac{m_C}{2} \left(r^2 + \bar{r}_0^2 \right) \tag{4}$$

where $\bar{r}_0$ is the inner radius of the coiling drum and r is the outer radius given in Eq. (2). The potential energy is

$$V_C = \frac{c_C}{2} \left[\left(x_W - x_{W0} \right)^2 + \left(y_W - y_{W0} \right)^2 \right] - m_C g y_S, \tag{5}$$

where c_C is the actual computed bending stiffness of the coiling drum. The controlled torque applied at the coiling drum is given by

$$M_T = M_0 + \alpha_C \left(\dot{s}_{L,D} - \dot{s}_L \right) + \beta_C \left(s_{L,D} - s_L \right) + \chi_C \left(\dot{x}_{WD} - \dot{x}_W \right) + \delta_C \left(x_{WD} - x_W \right), \tag{6}$$

where $s_{L,D}$, $\dot{s}_{L,D}$, x_{WD} and $\dot{x}_{WD}$ are the target values and α_C, β_C, χ_C and δ_C are defined parameters of the controller.

2.2 Model of the Moving Strip

With the axial speed of the strip on the left entry position $\dot{s}_L$ the longitudinal motion of the strip is defined by

$$u^*(\xi, t) = s_L + \left(s_R - s_L \right) \frac{\xi}{l_0}, \quad \dot{u}^*(\xi, t) = \dot{s}_L + \left(\dot{s}_R - \dot{s}_L \right) \frac{\xi}{l_0}, \tag{7}$$

where l_0 is the free length of the strip between the entry position and the drum, see Fig. 1, and ξ is the longitudinal coordinate. s_R and $\dot{s}_R$ are the kinematic variables for the coiled strip length and speed at the point on the coiling drum. For the transversal direction a Rayleigh-Ritz approximation

$$w_B^*(\xi,t) = \psi(\xi)q(t) \tag{8}$$

is used where the shape function

$$\psi(\xi) = \sin^2\left(\frac{\pi\xi}{l_0}\right) \tag{9}$$

is considered. The strip moves into the control volume at a fixed vertical position on the left boundary and the position where it attaches the drum is defined by the actual radius r and the vertical deflection y_W of the drum. The total transversal deflection is assumed by

$$w^*(\xi,t) = w_B^*(\xi,t) + (y_W - r)\,\frac{\xi}{l_0}, \tag{10}$$

where $w_B^*(\xi,t)$ is the bending deflection of the strip. The total velocity of the moving strip is

$$\dot{w}^*(\xi,t) = \dot{w}_B^*(\xi,t) + \frac{dw_B^*(\xi,t)}{d\xi}\dot{u}^*(\xi,t) + (\dot{y}_W - \dot{r})\,\frac{\xi}{l_0}. \tag{11}$$

The kinetic energy of the moving strip is computed by

$$T_S = \frac{1}{2}\int_0^{l_0} \rho A \dot{u}^*(\xi,t)^2 d\xi + \frac{1}{2}\int_0^{l_0} \rho A \dot{w}^*(\xi,t)^2 d\xi \tag{12}$$

resulting in

$$\begin{aligned} T_S = {} & \frac{m_S}{6}\left[\dot{s}_R^2 + \dot{s}_L\,(\dot{s}_L+\dot{s}_R) + 2\,(\dot{y}_W - \dot{r})^2\right] + \frac{m_S q}{2l_0}\left[\frac{3}{8}\dot{q}\,(\dot{s}_L - \dot{s}_R) - \dot{s}_R\,(\dot{y}_W - \dot{r})\right] \\ & + \frac{m_S\dot{q}}{4}\left(\frac{3}{4}\dot{q} + \dot{y}_W - \dot{r}\right) + \frac{\pi^2 m_S q^2}{12 l_0^2}\left[\left(\dot{s}_L^2 + \dot{s}_L\dot{s}_R + \dot{s}_R^2\right)\right] - \frac{m_S q^2}{32 l_0^2}\,(\dot{s}_L - s_R)^2 . \end{aligned} \tag{13}$$

With the strain in the strip $\varepsilon_S = \varepsilon_{xx} - zw'' + \frac{1}{2}w'^2$ the potential energy is given by

$$\begin{aligned} V_S = {} & \frac{1}{2}\int_0^{l_0}\left[EA\left(\frac{\partial u^*(\xi,t)}{\partial\xi}\right)^2 + EJ_S\left(\frac{\partial^2 w^*(\xi,t)}{\partial\xi^2}\right)^2\right] d\xi \\ & + \frac{1}{2}\int_0^{l_0} F_B\left(\frac{\partial w_B^*(\xi,t)}{\partial\xi}\right)^2 d\xi \end{aligned} \tag{14}$$

with the Youngs modulus E and the bending stiffness of the strip $J_S = \frac{bh^3}{12}$. Inserting the Rayleigh-Ritz approximations from Eqs. (8) and (9) we get

$$V_S = \frac{c_C}{2}\left(s_R - s_L\right)^2 + \frac{\pi^4 E J_S}{l_0^3} q^2 + \frac{\pi^2 F_B}{4 l_0} q^2 \tag{15}$$

The horizontal motion of the strip in longitudinal direction at the right position where it touches the coiling drum is defined by

$$s_R = \int_0^t r\dot{\varphi} dt + x_W - \frac{\pi^2}{l_0}\frac{q^2}{4} + a\sin\left(\varphi + \delta\right) \tag{16}$$

$$\dot{s}_R = r\dot{\varphi} + \dot{x}_W - \frac{\pi^2}{2l_0} q\dot{q} + a\dot{\varphi}\cos\left(\varphi + \delta\right) \tag{17}$$

for the Rayleigh-Ritz approximations and homogeneous initial conditions for s_R. φ is the rotation angle, a is the thermal deflection in the middle of the coiling drum and x_W is the horizontal deflection of the center of the rotating drum. For the Archimedian spiral of Eq. (2) the coiled length can be integrated to get

$$s_R = r_0\varphi + \frac{h\varphi^2}{4\pi} + x_W - \frac{\pi^2 q^2}{4 l_0} + a\sin\left(\varphi + \delta\right). \tag{18}$$

2.3 Extended Equations of Lagrange

The extended Equation of Lagrange for a non-material reference volume, which is given in Eq. (1) has to be used. In order to evaluate the surface integral terms corresponding to Fig. 2 the related velocities have to be defined. As some mass is transported into the mechanical system under consideration, we have to distinguish a material-fixed control volume (in this case a control surface) with the velocity vector

$$\mathbf{w}\left(t\right) = \begin{bmatrix} 0 \\ \dot{y}_W - \dot{r} \\ 0 \end{bmatrix} \tag{19}$$

and some material flowing through the boundary with the actual velocity vector of the mass

$$\mathbf{v}\left(t\right) = \begin{bmatrix} \dot{s}_L \\ \dot{y}_W - \dot{r} \\ 0 \end{bmatrix}. \tag{20}$$

The surface integral terms for these areas can be computed, where material flows through the surface with a constant speed within the surface. With these kinematic assumptions the integral terms can be evaluated which result from the extended Lagrange Equation (Eq. (1)) for each degree of freedom and result to

$$P_x = 0 \tag{21}$$

$$P_y = -\left(\dot{y}_W - \dot{r}\right)\rho \dot{s}_L A \tag{22}$$

$$P_\varphi = -\left(\dot{y}_W - \dot{r}\right)\tfrac{h}{2\pi}\rho \dot{s}_L A \tag{23}$$

$$P_{s_L} = \tfrac{(\dot{y}_W - \dot{r})^2 - \dot{s}_L^2}{2}\rho A \tag{24}$$

$$P_q = 0 \tag{25}$$

Finally the generalized forces which will be needed also in the extended Lagrange Equation (Eq. (1)) are given by

$$Q_x = \frac{\partial V}{\partial x_W} - d_x \dot{x}_W \tag{26}$$

$$Q_y = \frac{\partial V}{\partial y_W} - d_y \dot{y}_W \tag{27}$$

$$Q_\varphi = \frac{\partial V}{\partial \varphi} + M_D \tag{28}$$

$$Q_{s_L} = \frac{\partial V}{\partial s_L} - F_B \tag{29}$$

$$Q_q = \frac{\partial V}{\partial q} - d_q \dot{q} \tag{30}$$

It can be seen in the equations for the generalized forces, that some damping factors have been introduced with respect to the transversal motion of the coiling drum and the strip.

2.4 Equations of Motion for the Total Model

The derivation of the equations of motion based on the above equations for the kinetic and potential energy as well as the additional equations considering the flow through the boundary of the control volume the equations for the degrees of freedom of motion result. As they are lengthly equations they are not given here explicitly.

2.5 Semi-analytic Time-Integration Algorithm

The developed semi-analytic time-integration algorithm is based on the modal analysis of a modified dynamic system. For the resulting modally decoupled equations for the i-th degree of freedom

$$\ddot{q}_i + 2\zeta_i\omega_i\dot{q}_i + \omega_i^2 q_i = f_i(t) - \sum_{j=0, i\neq j}^{N} \left(\alpha_j q_j - \delta_j \dot{q}_j - \kappa_j \ddot{q}_j\right) \tag{31}$$

the solution is computed using the Duhamel-convolution integral with defined approximations of the evolution of the solution within a time-step. The resulting algorithm was analysed with respect to the numerical behaviour and it was found that it is superiour to the conventional known time-integration methods, see [5,14,15]. This semi-analytic algorithm was used for the time integration and with a suitable time step converged solutions are guaranteed.

3 Computed Results

For the derived mechanical model the solution was computed for different operation conditions and parametric studies have been performed. For the computation results presented in this contribution the parameters of the coiling drum are $l_0 = 5\,\mathrm{m}$, $\bar{r}_0 = 0.45\,\mathrm{m}$, $h = 10\,\mathrm{mm}$, $b = 0.5\,\mathrm{m}$, $E = 105\,\mathrm{kN/mm}^2$, $c_C = 10^7\,\mathrm{kN/m}$, $\rho = 7800\,\mathrm{kg/m}^3$, $m_0 = 1200\,\mathrm{kg}$. The controller parameters are given by $\alpha_C = 15\,\mathrm{kNs}$, $\beta_C = 10\,\mathrm{kN}$, $\chi_C = 10\,\mathrm{MNs}$ and $\delta_C = 10\,\mathrm{kN}$. The target parameters are $s_{L,D} = \dot{s}_{L,D}t$, $\dot{s}_{L,D} = 5,25\,\mathrm{m/s}$, $x_{WD} = 0\,\mathrm{m}$ and $\dot{x}_{WD} = 0\,\mathrm{m/s}$. In all computed examples it is guaranteed that there is a converged solution based on a suitable time step.

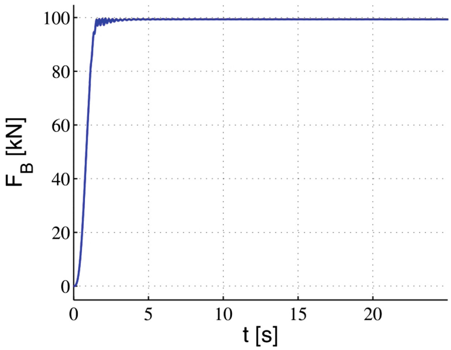

Fig. 3. First example: Strip tension force

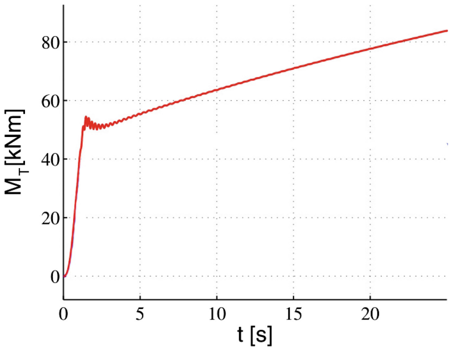

Fig. 4. First example: Computed torque at the coiling drum

For a first example a constant strip tension force of $F_B = 100\mathrm{kN}$ is applied as shown in Fig. 3. The load is increased within 1 s and is kept constant afterwards. With the given control parameters a steady operation is performed, resulting in a torque at the drum shown in Fig. 4. The torque increases proportional with the increasing outer radius of the coiling drum. The coiled strip length and the strip speed are given in Fig. 5. The corresponding outer radius of the coiling drum is shown in Fig. 6. The results for the horizontal position of the center of the coiling drum show small vibrations, see Fig. 7 and the mean value of the deflection results from the constant strip tension force. For the vertical position small vibrations are present as the drum is rotating and the gravity of the increasing mass results in an increasing weight of the drum which causes an increasing vertical delection y_W in Fig. 8. The small vibration amplitudes correspond to the non-homogeneous initial conditions and to the linear increase of the outer radius. It is mentioned that for the assumption of a step function of the outer radius according to $r = r_0 + h\lfloor\frac{\varphi}{2\pi}\rfloor$ high vibration amplitudes occur after every rotation. The corresponding computational results are shown in Fig. 9 for a sequence of Heaviside-functions, where the high fluctuations of the strip tension force can be seen. Some additional effort is necessary for the computation of this case as negative strip tension forces are not permitted. Due to the coiling process and the design of the coiling drum the outer radius shows some more complicated shapes which have been analyzed.

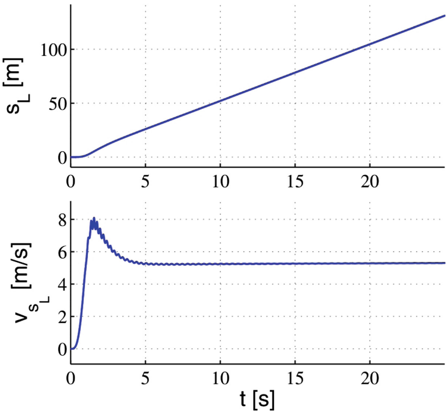

Fig. 5. First example: Coiled strip length and strip speed

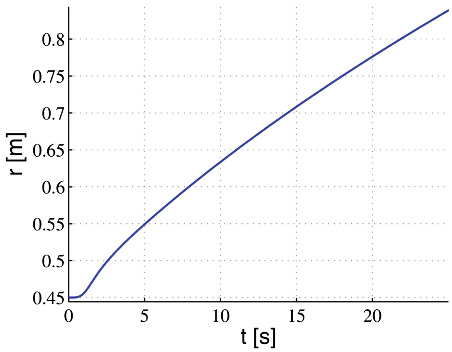

Fig. 6. First example: Outer radius of the coiling drum

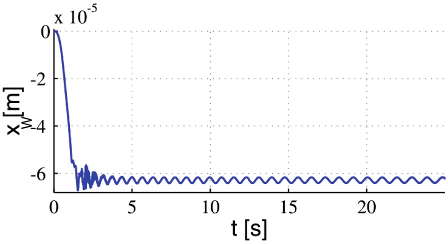

Fig. 7. First example: Horizontal position of the center of the coiling drum

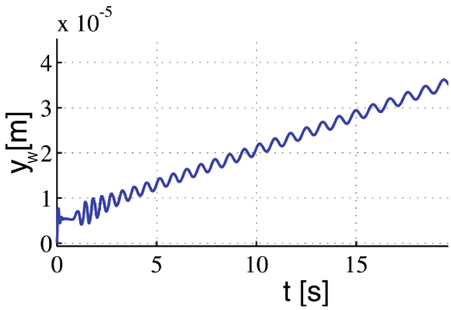

Fig. 8. First example: Vertical position of the center of the coiling drum

For a second example the strip tension force is $F_B = F_{B0}\left(1 + \frac{\sin(\pi t/2)}{2}\right)$ with $F_{B0} = 50$kN and all the other parameters are kept unchanged. The computation is carried out and the controlled torque at the drum is shown in Fig. 10. From the results of the transversal strip vibrations in Fig. 11 the coupling effect with the varying frequency and amplitude is shown. In Figs. 12 and 13 the results for the motion of the center of gravity of the coiling drum are drawn for the horizontal and vertical direction. The horizontal motion is caused by the varying strip tension force and the vertical motion is induced by the variation of the strip

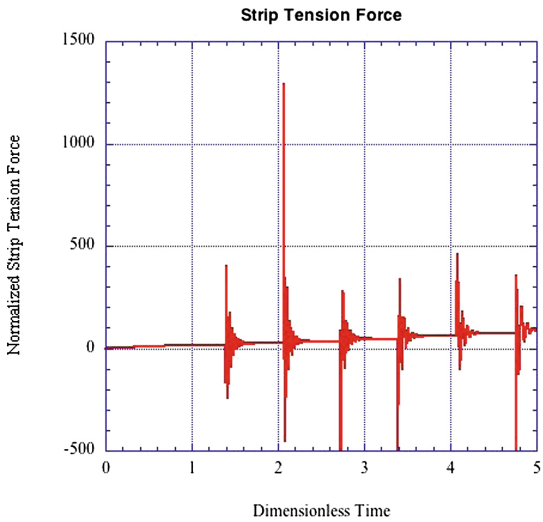

Fig. 9. First example: Normalized strip tension force for a radius function with a sequence of Heaviside-functions

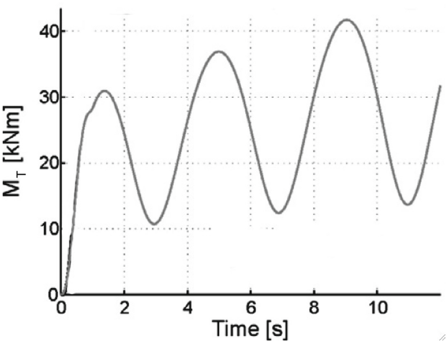

Fig. 10. Second example: Torque at the coiling drum

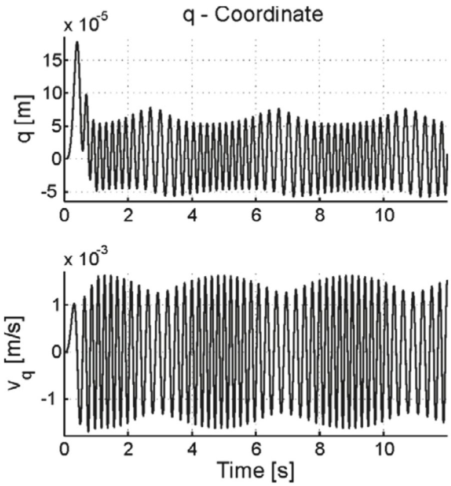

Fig. 11. Second example: Amplitude and velocity of transversal motion of the strip

tension force. In the vertical position it can be seen that the influence on the weight is not considered in this example.

For the third example the parameters for the mechanical model of Fig. 1 are the same, except for $\bar{r}_0 = 0.4$ m and $F_B = 50$ kN, which are now kept constant. The computed results are shown for two different thermal deflections of

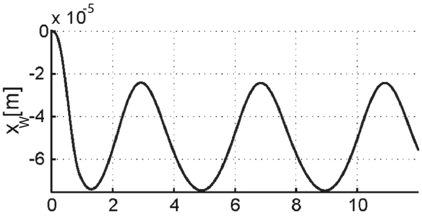

Fig. 12. Second example: Horizontal position of the center of the coiling drum

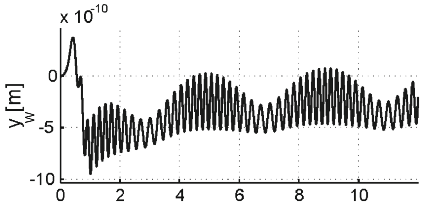

Fig. 13. Second example: Vertical position of the center of the coiling drum

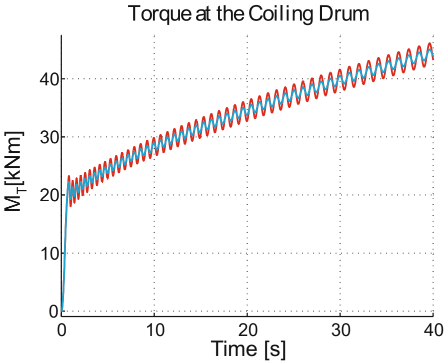

Fig. 14. Third example: Computed torque at the coiling drum for $a = 0.1$ (blue) and 0.23 mm (red)

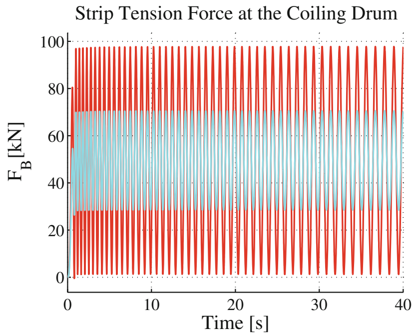

Fig. 15. Third example: Computed strip tension force for $a = 0.1$ (blue) and 0.23 mm (red)

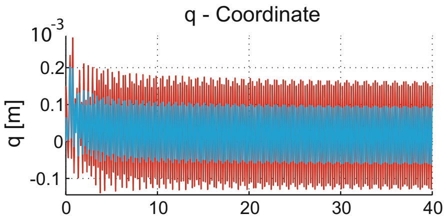

Fig. 16. Third example: Moving strip - Transversal oscillations for $a = 0.1$ (blue) and 0.23 mm (red)

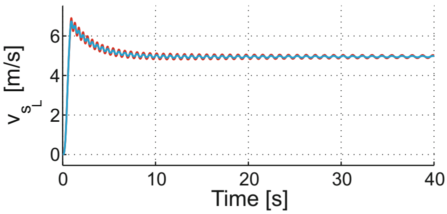

Fig. 17. Third example: Computed axial strip speed for $a = 0.1$ (blue) and 0.23 mm (red)

$a = 0.1$ mm and $a = 0.23$ mm. Figure 14 shows the computed torque and in Fig. 15 the strip tension force is shown. If $a = 0.23$ mm the minimum strip tension force is computed to be $F_B \geq 0$ N. The transversal deflection of the moving strip is given in Fig. 16 which is a results of the strip tension force F_B and the motion of the coiling drum with the thermal deflection a. For the higher excitation amplitude of the thermal deflection the transversal oscillations of the strip are higher. The excitation frequency and the frequency of transient vibration are very different. In Fig. 17 the axial speed of the strip is shown as there is a constant F_B maintained at the left boundary. This result is similar to that for the first example, see Fig. 5, but with a much smaller strip tension force and a thermal deflection of the shaft of the coiling drum. Different fluctuations in the axial strip speed can be seen which are caused by the two different thermal deflection values.

4 Conclusion

A mechanical model with a variable mass and varying parameters of a coiling process was derived. The simulation results for three different examples show that for a steady state production process with a constant axial speed the vibration amplitudes are very small. For the non-linear dynamic system with variable mass vibrations are computed for given forces at the left entrance boundary and a controlled torque. For a defined variation of the strip tension force at the entrance the vibration amplitudes are higher than for a constant strip tension force. The frequency and amplitude for the transversal strip oscillation depend on the strip tension force. The influence of the process parameters are studied to reduce the vibrations and results are given for two different thermal deflection values.

Acknowledgments. Support of this work in the framework of the Comet-K2 Linz Center of Competence in Mechatronics (LCM), Area 2, MECON-Complete mechanical systems and automatic control, is gratefully acknowledged.

References

1. Irschik, H., Holl, H.J.: The equations of lagrange written for a non- material volume. Acta Mech. **153**(3–4), 231–248 (2002)
2. Ziegler, F.: Mechanics of Solids and Fluids, 2nd edn. Springer Verlag, New York (1998)
3. Irschik, H., Holl, H.J.: Lagrange's equations for open systems, derived via the method of fictitious particles, and written in the Lagrange description of continuum mechanics. Acta Mech. **226**, 63–79 (2015)
4. Irschik, H., Holl, H.J.: Mechanics of variable-mass systems - part 1: balance of mass and linear momentum. Appl. Mech. Rev. **57**(2), 145–160 (2004)
5. Holl, H.J.: A time-integration algorithm for time-varying systems with non-classical damping based on modal methods. In: Wicks, A.L. (ed.) Proceedings of the 15th International Modal Analysis Conference, 3–6 February 1997, Orlando, pp. 1558–1564. Society for Experimental Mechanics (1997)
6. Holl, H.J., Belyaev, A.K., Irschik, H.: A time integration algorithm for nonlinear rotordynamic systems with time-varying parameters. In: Muszynska, A. (ed.) Proceedings of the Seventh International Symposium on Transport Phenomena and Dynamics of Rotating Machinery (7th ISROMAC), 22–26 February 1998, Honolulu, vol. B, pp. 930-940. Bird Rock Publishing House (1998)

7. Holl, H.J., Finstermann, G., Mayrhofer, K., Irschik, H.: Vibration simulation of the Steckel mill strip coiling process. In: Mang, H.A., Rammerstorfer, F.G., Eberhardsteiner, J. (eds.) Proceedings of the Fifth World Congress on Computational Mechanics (WCCW V), 7–12 July 2002, Wien. Vienna University of Technology, Austria (2002). http://wccm.tuwien.ac.at
8. Holl, H.J., Finstermann, G., Mayrhofer, K., Irschik, H.: Nonlinear vibrations during the pass in a Steckel mill strip coiling process, In: Radons, G., Neugebauer, R., Wiley-VCH, (eds.) Nonlinear Dynamics of Production Systems, Weinheim, pp. 305–316 (2004)
9. Holl, H.J., Hammelmüller, F.: Simulation of a coiling process with thermal deflection of the drum. In: Ziegler, F., Heuer, R., Adam, C. (eds.) Proceedings of the Sixth International Congress on Thermal Stresses (TS2005), Vienna University of Technology, Vienna, Austria, 26–29 May 2005, vol. 1, pp. 377–380. Schriftenreihe der Technischen Universität Wien (2005)
10. Cveticanin, L.: The influence of the reactive force on the motion of the rotor on which the strip is winding up. J. Sound Vib. **167**, 382–384 (1993)
11. Cveticanin, L.: Dynamics of Machines with Variable Mass. Gordon and Breach Science Publishers, Philadelphia (1998)
12. Holl, H.J., Hammelmüller, F.: Zum Einfluss einer veränderlichen Exzentrizität auf die Schwingungen beim Wickelprozess 10. In: Liebich, R. (ed) Internationale Tagung Schwingungen in Rotierenden Maschinen X (SIRM X on CD-Rom), 25–27 February 2013, Berlin, paper-ID ABS-218, p. 10 (2013)
13. Hammelmüller, F., Holl, H.J.: The effect of variable eccentricity onto the oscillations in a coiling process. In: PAMM, vol. 3, no. 1, pp. 104–105 (2003)
14. Holl, H.J.: An efficient semi-analytic time-integration method with application to non-linear rotordynamic systems. Comput. Mech. **26**(4), 362–375 (2000)
15. Holl, H.J.: A modal-based substructure method applied to nonlinear rotordynamic systems. Int. J. Rotating Mach. Article ID 313526, 8 p. (2009). https://doi.org/10.1155/2009/313526